Measuring the height of steps on MgO cubes using Fresnel contrast in a scanning transmission electron microscope

C.B. Boothroyd and C.J. Humphreys

Department of Materials Science and Metallurgy, University of Cambridge, Pembroke Street, Cambridge CB2 3QZ, UK

Dedicated to Professor John M. Cowley on the occasion of his seventieth birthday

The possibility of using Fresnel (or phase) contrast in a scanning transmission electron microscope as a means of measuring the heights of steps on the surface of MgO smoke cubes is examined. It is shown that once the microscope parameters are known it is possible to match the intensities of the Fresnel fringes quantitatively with multislice simulations for step heights of the order of a few monolayers on a cube of thickness 44 nm.

1. Introduction

The surface of MgO smoke cubes is very sensitive to damage by the electron beam in a scanning transmission electron microscope (STEM). When looked at for long periods at low magnification (e.g. 100k) surface steps arranged in rectangular patterns, which are most easily seen slightly out of focus, form and move about. At higher magnifications (e.g. 5M), corresponding to higher dose rates, material is rapidly cut away in the area scanned by the beam leaving a surface on which no steps are visible, even if many steps were present initially [1,2]. If the dose rate is increased to the limit by leaving the beam stationary then a hole can be drilled through an 80 nm thick cube in ~ 120 s [3]. The MgO surface is also sensitive to impurities such as water and Al; for example, after evaporating a ~ 10 nm layer of Al onto MgO, Cowley et al. [4] found that steps as large as 20 nm were formed. In order to understand the formation and movement of steps on MgO surfaces it is necessary to know how steps are made visible and thus under what conditions an atomic height step can be seen.

Surface steps can be seen in either the transmission electron microscope (TEM) or the STEM by reflection microscopy, by diffraction contrast or by out of focus contrast. Reflection microscopy [5,6] is possibly the most sensitive technique but is unsuitable in our case for observing steps at the bottom of holes. In the TEM single atomic layer steps on MgO have be seen clearly by diffraction contrast, typically in a weak-beam condition [7,8] when terraces of constant thickness appear as areas of uniform optical density, but the specimen must be accurately oriented and at optimum thickness and in addition long exposures are required. Alternatively steps can be made visible by Fresnel or phase contrast by viewing slightly out of focus [9–11]. In this method the specimen orientation is not as critical provided it is away from a Bragg condition, but only the step edges are made visible so the step height is more difficult to quantify and it is not possible to be sure that atomic steps are visible. In this study a STEM was used for damaging the MgO crystals and thus also for taking the images, although from the image resolution point of view a TEM would have been better. In the absence of a TEM with an imaging filter the STEM has the advantage that the images can be energy filtered. In order to study the surface step structure on MgO and how this structure changes under electron

irradiation it is necessary to quantify both the diffraction contrast and the Fresnel contrast produced in a STEM by steps on MgO cubes and thus be able to compare the step heights measured by both methods.

2. Microscope parameters

The microscope used was a VG HB501 STEM attached to a Link AN10000 computer allowing direct acquisition of energy filtered 256 pixels square 12 bit resolution images with an exposure time of about 1 min. These were subsequently transferred to a microVAX running the Semper image processing program for analysis. Heavy use was made of the reciprocity between STEM and TEM images [12] for multislice image simulations and images were acquired under TEM-type conditions of low beam convergence, i.e. small collector aperture (50 μm, corresponding to 0.66 mrad

radius) and small spot size (condenser lens 1 at 21).

In order to do the multislice simulations it was first necessary to determine the microscope parameters used. This was done by taking a digitised through focal series of images of the amorphous carbon support film near the MgO cubes and calculating their "optical" diffractograms (fig. 1). From figs. 1a to 1e it is possible to determine the objective focal increments (150 nm for the "fine" lens control) and confirm that the spherical aberration constant, C_s, is 3.1 mm. From the highest defoci it is found that a convergence of 0.6 mrad (RMS of equivalent gaussian) fitted the diffractograms best, which agrees well with the angular radius of the 50 μm collector aperture of 0.66 mrad, despite the simulations assuming a gaussian rather than a top hat profile.

From the near-focus diffractograms a RMS focal spread of 50 nm fitted best, but its meaning is more difficult to interpret. For an illumination
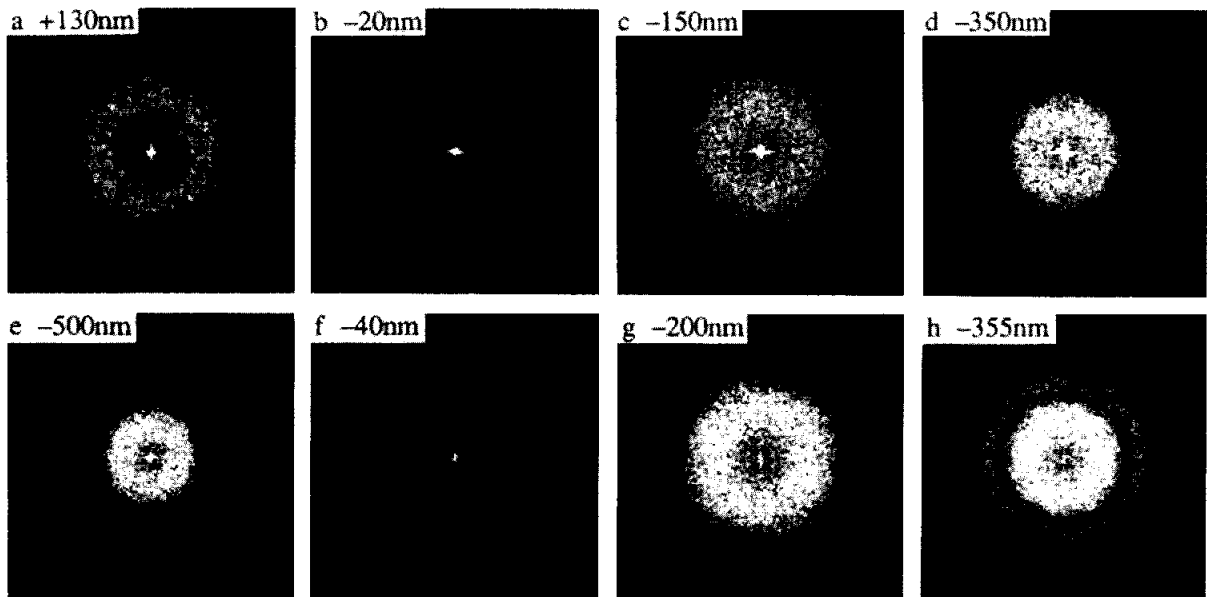

Fig. 1. "Optical" diffractograms calculated from images of amorphous carbon acquired digitally using the HB501 STEM. The objective aperture diameters used were 150 μm for (a)–(e) (corresponding to 23 mrad radius or a minimum spacing transferred of 0.16 nm) and 50 μm for (f)–(h) and all subsequent images (corresponding to 7.6 mrad radius or a minimum spacing of 0.49 nm). The scale of the figures is such that the edge of each diffractogram corresponds to 7.6 mrad and the defocus is shown at the top of each diffractogram. Black corresponds to zero intensity and white to 0.002 on a scale where the mean intensity of the original images was scaled to 1.

energy spread of 0.3 eV the focal spread would be ~ 10 nm, thus the observed focal spread must derive from objective lens instabilities or the effects of specimen vibration and finite spot size, all of which have similar effects on the optical diffractogram to focal spread. Although it would be interesting to know the source of the focal spread, for the purpose of these calculations all that matters is that the parameters used make the transfer functions match the diffractograms over the defocus range used in the subsequent simulations. Figs. 1f to 1h show diffractograms similar to figs. 1b to 1d but with the 50 μm objective aperture inserted as used in all subsequent figures. It can be seen that small additional aberrations are introduced presumably due to the objective aperture charging, and that there is transfer out to higher frequencies, probably because with the 50 μm aperture there is much less specimen irradiation during the exposure and hence less damage to the carbon film.

3. Image simulations

Given that the MgO cubes are in a weakly diffracting condition, i.e. there are no thickness fringes visible at the sloping edges of the cubes and the images are at low (i.e. not atomic) resolution (the 50 μm objective aperture transfers spacings down to 0.49 nm) a continuum multislice simulation was used, where only the mean potential (V_0) of the crystal and not the atoms is considered [13]. A full atomistic simulation would require the exact crystal tilt to be known (it was roughly 10° from [001] in the direction of [110]) and, given the inaccuracies of the approximations used in multislice programs to represent tilts a long way from zone axes, may not be particularly accurate anyway.

In these calculations we simulate a one-dimensional crystal of MgO with a step of height n monolayers (each monolayer is 0.21 nm high) on its top surface, i.e. the surface furthest away from the objective lens in both TEM and STEM. In fact, it makes little difference whether the step is on the top or the bottom surface, apart from a shift in the position of zero defocus of the step by the thickness of the crystal. The slice thickness in the multislice calculation is equal to one monolayer, so to represent a step of height n monolayers the first n slices consisted of a one-dimensional unit cell, half of which contained MgO and half of which contained vacuum, thus representing two steps, one in the middle of the cell and one at the edge due to periodic continuation. For the rest of the calculation, up to the thickness of the MgO crystal (44 nm), the unit cell contained
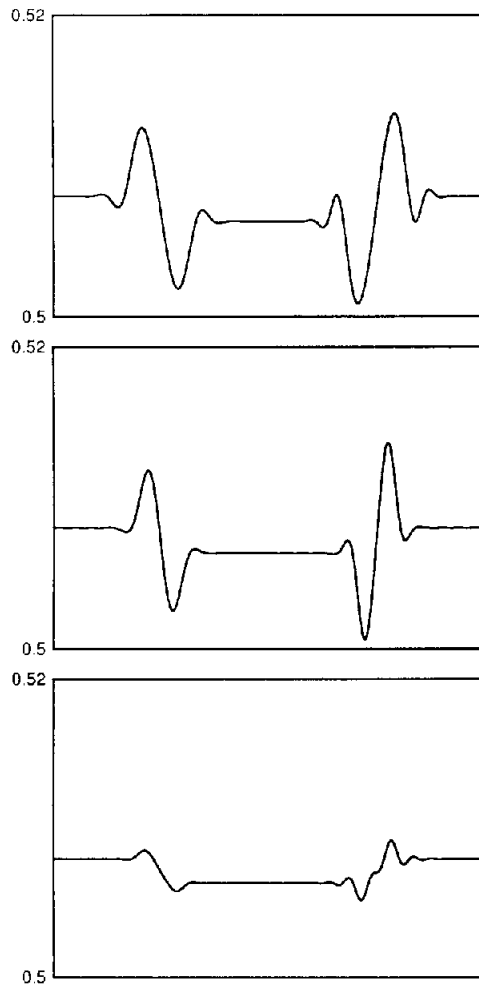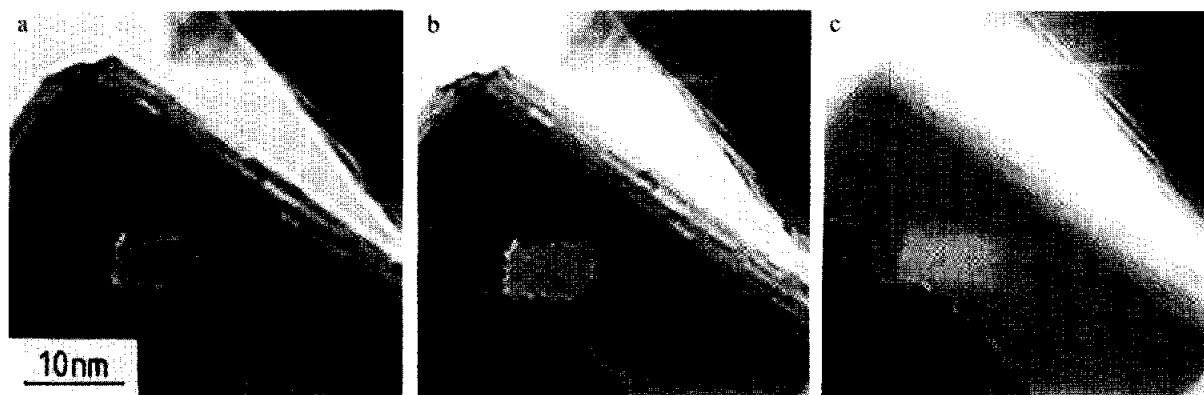

Fig. 2. Simulations for a step diffuse over ~ 2 nm (left) and an abrupt step (right), both of monolayer (0.21 nm) height. The defocus values, −370 nm (top), −220 nm (middle) and −70 nm (bottom) are measured relative to the bottom of the 44 nm thick MgO crystal. Each image is 12.8 nm wide.

Fig. 3. Series of images from underfocus to near focus with a focal imcrement of 150 nm of an MgO cube containing a rectangular damaged area. The intensities here have not been normalised.

entirely MgO. Since this is a continuum calculation, MgO is represented in the unit cell by its mean forward-scattering potential $V_0 = 13$ V and its imaginary part $V_0' = 0.84$ V. V_0 is the most important parameter since the contrast in the calculated images is proportional to V_0, and is also the most difficult to determine. Spence [14] lists experimentally determined values of V_0 for MgO varying from 12.3 to 16 V, while a theoretical calculation corrected for bonding using the method of Ross and Stobbs [15] gives a value of ~ 13 V and this is the value for V_0 which has been used here. To take account of diffraction and inelastic scattering, absorption was introduced by fitting the imaginary potential V_0' to

give the correct reduction in intensity at a known thickness. After the multislice part of the simulation the objective lens parameters were allowed for using the Semper mutual transfer function routine "iit".

4. Results

The degree of abruptness of a step can have a large effect on the Fresnel contrast simulated, so simulations for an abrupt monolayer step and a step diffuse over about 2 nm are shown in fig. 2. It can be seen that the major difference between the profiles is that the abrupt step has more
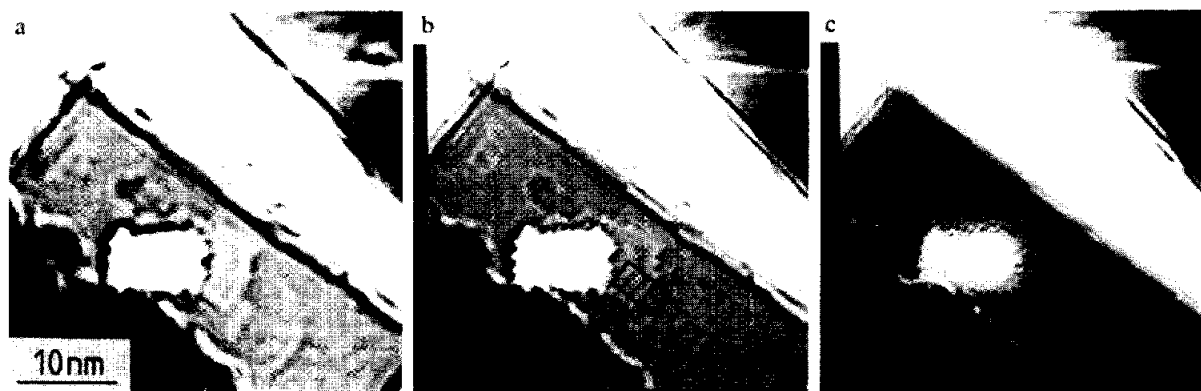

Fig. 4. Images as fig. 3 but after intensity normalisation so 0 corresponds to zero intensity and 1 corresponds to the incident intensity. The contrast has been stretched to show the steps by displaying with 0.45 as black and 0.65 as white.

fringes in the image at −70 nm defocus whilst there is only a small decrease in the Fresnel fringe heights of the images at larger defoci. The diffuse step is taken to be a better representation of a real step as a row of alternating Mg and O atoms will be slightly diffuse when averaged along its length and not surprisingly the diffuse images match the experimental images shown later bet-
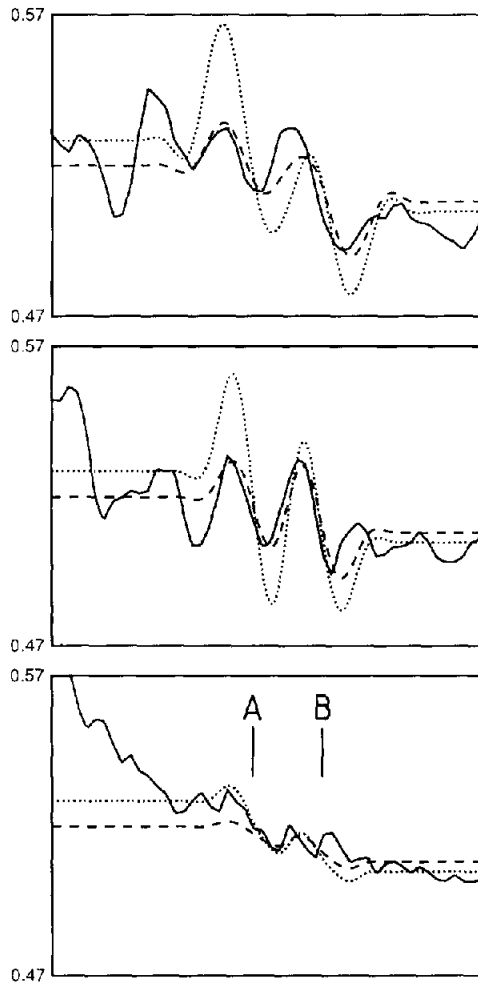

Fig. 5. The solid line is the area marked "5" in fig. 4b averaged along the length of the fringes with the two steps simulated marked A and B. The dotted line is a simulation for step heights of A 1.7 nm (8 monolayers) and B 1.3 nm (6 monolayers), and the dashed line is a simulation for step heights of A 0.6 nm (3 monolayers) and B 0.8 nm (4 monolayers). The defoci are top −370 nm, middle −220 nm and bottom −70 nm and each image is 7.75 nm wide.
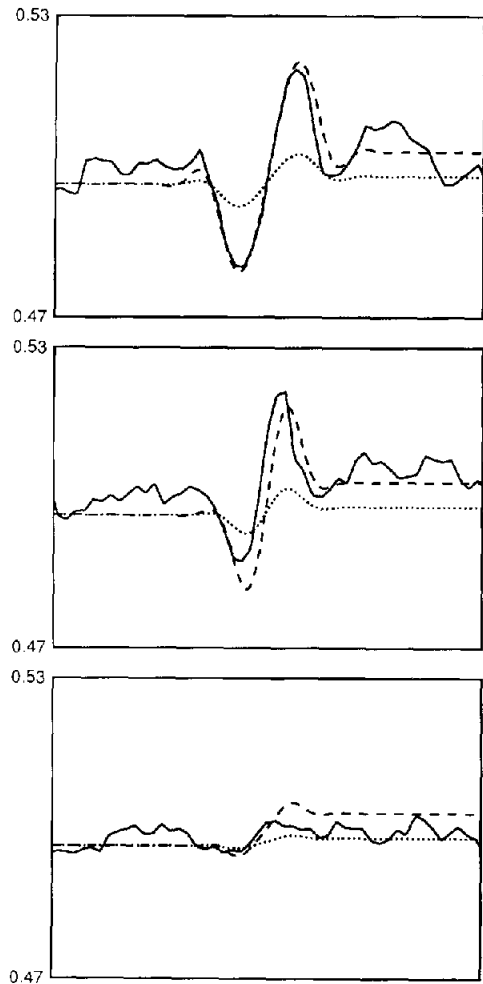

Fig. 6. As fig. 5 except the solid line is the area marked "6" in fig. 4b averaged along the length of the fringes. The dotted line is a simulation for a step height of 0.21 nm (1 monolayer) and the dashed line 0.84 nm (4 monolayers).

ter near focus than the abrupt images. The component of the specimen tilt in the [100] direction (∼ 7°) has only a comparatively small (e.g. ∼ 0.2 nm for 8 monolayer step) effect on the step diffuseness. Any errors in the degree of abruptness will have a small effect on the heights of the fringes at −220 and −370 nm as can be seen from the top two images of fig. 2.

A typical series of images of a MgO cube taken with a focal increment of 150 nm is shown in fig. 3. To extract quantitative fringe profiles from these images a black level picture must also

be taken with no electrons incident on the detector (usually done by setting the energy loss spectrometer to collect electrons of energy a few hundred eV above 100 kV) then each image can be normalised by subtracting the black level derived from the mean of the black level image and scaling the region containing no specimen to a value of 1. Each image was aligned by cross correlating with fig. 3a to correct for specimen drift. Suitable regions could be chosen by enhancing the contrast as in fig. 4. It can be seen especially from fig. 4c that the major source of noise is the random variations in the beam current which give rise to horizontal streaks. Attempts were made to remove this noise by dividing each image by either the objective or virtual objective aperture currents but little improvement was found.

Finding suitable fringes for analysis proved difficult – the fainter fringes tend to be obscured by other fringes on both the top and bottom surfaces of the cube and tend to move between images due to the MgO damaging during each exposure. The areas extracted and averaged along the length of the fringes (figs. 5 and 6) are thus from areas containing some of the stronger fringes and are marked on fig. 4b. The step heights can now be estimated from the change in the mean intensity level across each step in the "in focus" image of fig. 5 and correspond to 1.7 nm for step A and 1.3 nm for step B. It would have been desirable to obtain a weak-beam image to enable

the step heights to be measured more accurately but the amount of damage the crystal would have suffered during this process would have changed the step structure beyond all recognition. Simulations for 1.7 and 1.3 nm steps are shown with dotted lines in fig. 5. It can be seen that they overestimate the fringe contrast by a factor of about 2 and that the simulations shown with the dashed line for step heights of 0.6 and 0.8 nm provide better fits for the Fresnel fringes in the -370 and -220 nm defocus images.

The single fringe shown in fig. 6 has a step height of 0.25 nm corresponding to just 1 monolayer (0.21 nm) estimated from the mean intensity levels on either side of the steps. However, simulations for a monolayer step show that this is an underestimate (dotted line in fig. 6) and that a 0.8 nm (4 monolayers) step fits the Fresnel contrast much better (dashed line). The inaccuracy is not surprising as there is overlap of fringes from other steps into the area analysed and the noise level in the in-focus image is about the same as the difference in intensity across the step.

Considering the area of the cube that has been planed by scanning the beam at a magnification of about 10M for a few minutes shown in fig. 7, it can be seen that there is a zig-zag step running from top to bottom near the left edge of the planed area, with the area to the left of the step thinner, and most easily seen in fig. 7b. This is where the beam rests momentarily during flyback at the beginning of a scan line and so is slightly
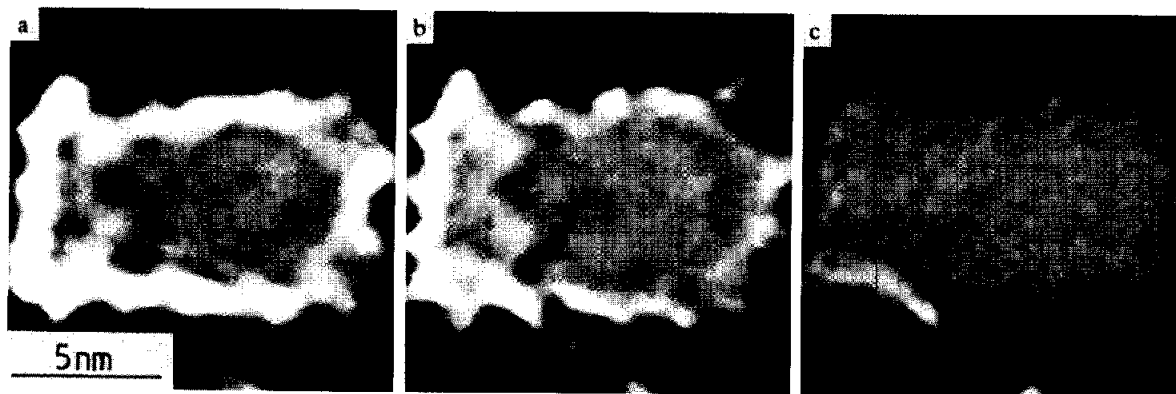

Fig. 7. Enlargements of the planed area of the images shown in fig. 4 with 0.5 as black and 0.75 as white.

more heavily damaged. In the rest of the planed area there is a faint criss-cross pattern that probably represents single monolayer steps, however the planed area is too small and the fringes too faint to allow for quantitative analysis.

5. Conclusions

It has been shown that STEM images can be quantified once the lens parameters are known and matched *quantitatively* to multislice simulations. For the resolution used here only a simple continuum model is needed to get good fits to the Fresnel fringes and the major source of error is in determining the mean potential V_0. Step heights measured by diffraction contrast and Fresnel fringe contrast agree fairly well with the diffraction contrast estimates of step height for the two areas analysed falling either side of the Fresnel fringes estimates. The major sources of error are contributions from fringes from nearby steps to the mean intensity levels on either side of each step and the background noise level in the images. Fresnel fringe measurements thus provide an important way of measuring surface step heights which we will be applying to the study of how atoms are removed from planed areas.

References

[1] T.J. Bullough, C.J. Humphreys and R.W. Devenish, Mater. Res. Soc. Symp. Proc. 157 (1990) 323.

[2] R.W. Devenish, T.J. Bullough, P.S. Turner and C.J. Humphreys, in: EMAG-MICRO 89, Eds. P.J. Goodhew and H.Y. Elder, IOP Conf. Ser., Vol. 98 (IOP, Bristol, 1990) p. 215.

[3] P.S. Turner, T.J. Bullough, R.W. Devenish, D.M. Maher and C.J. Humphreys, Phil. Mag. Lett. 61 (1990) 181.

[4] J.M. Cowley, Prog. Surf. Sci. 21 (1986) 209.

[5] H.-J. Ou and J.M. Cowley, Ultramicroscopy 22 (1987) 207.

[6] P.A. Crozier, M. Gajdardziska-Josifovska and J.M. Cowley, Microsc. Res. Tech. 20 (1992) 426.

[7] G. Lehmpfuhl and C.E. Warble, Ultramicroscopy 19 (1986) 135.

[8] K. Kambe and G. Lehmpfuhl, Optik 42 (1975) 187.

[9] A.F. Moodie and C.E. Warble, Phil. Mag. 16 (1967) 891.

[10] S. Iijima, Optik 47 (1977) 437.

[11] C. Boulesteix, C. Colliex, C. Mory, D. Renard and B. Yangui, J. Microsc. Spectrosc. Electron. 3 (1978) 185.

[12] C. Colliex, A.J. Craven and C.J. Wilson, Ultramicroscopy 2 (1977) 327.

[13] J.N. Ness, W.M. Stobbs and T.F. Page, Phil. Mag. A 54 (1986) 679.

[14] J.C.H. Spence, in: Electron Diffraction Techniques, Vol. 1, Ed. J.M. Cowley (OUP, Oxford, 1992) p. 360.

[15] F.M. Ross and W.M. Stobbs, Phil. Mag. A 63 (1991) 37.